DOI: 10.1002/ejic.201100447

Structural Investigation of a Fully Ordered *closo*-Ge_9^{2-} Cluster in the Compound $[K^+(2,2,2\text{-crypt})]_2Ge_9^{2-}$

Josefin Åkerstedt,[a] Simeon Ponou,[b] Lars Kloo,[a] and Sven Lidin*[b]

Dedicated to Professor John D. Corbett on the occasion of his 85th birthday

Keywords: Germanium / Zintl anions / Cluster compounds / X-ray diffraction / Cryptands

$[K^+(2,2,2\text{-crypt})]_2Ge_9^{2-}$ containing the deltahedral Zintl anion Ge_9^{2-} has been isolated from a solution of K_4Ge_9 in ethylenediamine in the presence of 2,2,2-crypt, intended as an intermediate in mixed-cluster synthesis. The subsequent crystallographic characterisation shows the *closo*-Ge_9^{2-} cluster unit to be tricapped trigonal-prismatic with a symmetry very close to D_{3h}. Each Ge_9^{2-} unit is surrounded by two 2,2,2-crypt units, each with a chelated K^+ cation, viz. $[K^+(2,2,2\text{-crypt})]$. The structure characterisation of this ordered Ge_9^{2-} cluster is surprisingly enough the first one reported. A chemical bonding analysis reveals two local minima of D_{3h} symmetry, with that of lowest energy being highly similar to that resulting from the crystallographic analysis of low-temperature data. The cluster interaction scheme is based on highly delocalised bonding.

Introduction

Naked germanium clusters have been reported in several alkali metal compounds; Ge_4^{4-} units form the equimolar compounds first denoted as KGe,[1] and Ge_9^{4-} was found in Cs_4Ge_9[2] and in a number of compounds stabilised by large, sequestered counter-cations. The earliest structurally characterised example originates from the work of Corbett and co-workers, the compound $(\text{crypt-}K^+)_6Ge_9^{2-}Ge_9^{4-}\cdot 2.5\text{en}$.[3] In this compound, the Ge_9^{4-} unit is accompanied by what is reported to be a Ge_9^{2-} unit, although the geometry of this second cluster is odd and displays some unexpectedly long Ge–Ge distances. The crypt-cation (potassium) preparative routes of synthesis also produced the first reported sources of crystalline Ge_9^{3-}[4] and Ge_5^{2-}.[5] Later, extensive oligomeric/polymeric chemistry of Ge_9 clusters was developed, first by the synthesis of $(Ge_9)_2$ dimers,[6] infinite polymeric chains $(Ge_9)_\infty$[7] and then trimers[8] and tetramers.[9] This development is well covered in several papers and reviews.[10–16] An early report of a Ge_{10}^{2-} cluster[17] has been challenged as erroneous[18,19] on the grounds that the extensive disorder in the structure precludes an exact assessment of the composition and structure, complemented with arguments that the charge balance is more naturally achieved by a Ge_9^{2-} unit. Surprisingly, there is to date no published single-crystal determination of the expected archetypical, tricapped trigonal-prismatic Ge_9^{2-} unit. Very recently, Sevov and Rios reported a structurally well characterised Ge_{10}^{2-} cluster as a “ligand” to $Mn(CO)_4^-$.[20]

The characterisation of main-group clusters presents many challenges. First, many systems yield only crystals of poor quality, and the subsequent structural analysis exhibits phenomena such as partial amorphicity and twinning. This is partly compensated for by the use of low-temperature routes of synthesis. However, even if good-quality crystals are obtained, the compounds isolated often display superstructures and static as well as dynamic disorder. It is quite common that even the number of atoms involved cannot be unambiguously determined from the structural data at hand. In such cases, being the rule rather than the exception, an accurate elemental analysis together with the demand for electroneutrality can be of good help. However, and this is the second main challenge, accurate elemental analysis for these types of compounds is difficult to obtain since they are highly sensitive to moisture and oxygen, and there are many cases in the literature in which the proposed clusters later turned out to have compositions and charges different from what was originally assumed. However, we do not want to point the finger since we have certainly made such a mistake ourselves in the past (a proposed Sb_5^{3+} cluster was later shown to be Sb_8^{2+}).[21,22] An additional challenge is that even if the composition and structure are correct, they cannot be unambiguously rationalised in terms of electron bookkeeping rules,[23] because the structural fluxionality of the clusters is too high. The present work, employing a detailed structural analysis of high-quality crystals obtained from organic solutions at low tem-

---

[a] Division of Inorganic Chemistry, Royal Institute of Technology, 10044 Stockholm, Sweden
[b] Division of Polymer and Materials Chemistry, Lund University, 22100 Lund, Sweden

Supporting information for this article is available on the WWW under http://dx.doi.org/10.1002/ejic.201100447.

perature, is to attempt to iron out some of the ambiguities mentioned above.

The standard procedure for producing Ge_9^{3-} clusters in solution was used, and from the reaction mixture high-quality crystals of $[K^+(2,2,2\text{-crypt})]_2Ge_9^{2-}$ were isolated. We herein report the thorough crystallographic evaluation of the *closo*-Ge_9^{2-} cluster structure along with results from Raman spectroscopy and quantum chemical calculations. The results presented show this to be the first structurally properly determined Ge_9^{2-} cluster, and they confirm the identity of this compound. The results obtained clearly show that it is sometimes worthwhile to reassess old results.

Results and Discussion

The reaction resulting in the isolation of $[K^+(2,2,2\text{-crypt})]_2Ge_9^{2-}$ from a solution originally intended for further synthetic modification, follows the standard procedure reported in the literature for these types of compounds. However, the quality of the crystals produced in the reactions reported within this work appears to exceed the quality of the previously isolated and investigated crystals of this system. Hence, the single-crystal X-ray diffraction investigation carried out on this system proved rewarding.

The structure determined at 100 K is fully ordered. It is interesting to note that it contains two distinct objects with local threefold symmetry, but their threefold axes are not parallel. The composition is absolutely unambiguous: For each *closo*-Ge_9^{2-} unit, there are two cryptand units $[K^+(2,2,2\text{-crypt})]$. The geometry of the *closo*-Ge_9^{2-} unit is very well defined in the refinement. The tricapped trigonal prism contains two distinct types of narrowly defined Ge–Ge distances (cf. Figure 1): short distances (ca 2.56 Å) can be observed between the atoms that cap the square faces of the trigonal prism and the atoms that form the vertices of the prism itself. Longer distances may be observed between these vertices (ca 2.73 Å). Knowing the structure of the ordered cluster, it is easy to devise a model for the 250 K structure, which is consistent with the low-temperature structure (cf. Figure 2). By starting from a model derived directly from the diffraction data, with the occupancies of all Ge positions refined, an occupancy of 63 % for Ge1 and occupancies of 26, 28, 36 and 42 %, for Ge2–Ge5, respectively, are obtained. If these positions represented complete rotational disorder about the triad, we would expect 1/3 occupancy for all positions, but the clusters overlap pairwise on the position of Ge1, and hence the occupancy of this is 2/3. Upon implementing these restrictions, a solution that agrees equally well with the data as does the original unrestricted model can be obtained. It is clear from the X-ray data that the compound under investigation is the same as that synthesised by Belin.[17] The structure refined from the 250 K data set is very similar to that of Belin, and invoking Belin's model on our 250 K data produced a refinement result of very similar quality to our own. The data set measured at 100 K is distinctly different and indicates that the compound undergoes an order/disorder transition between 250 K and 100 K. The change is easily seen in the single-crystal data, but it is too subtle to be monitored by using powder methods. Hence it was not possible to identify the transition temperature with any accuracy.

In order to further investigate the isolated product, Raman spectra were recorded from the crystalline solid of $[K^+(2,2,2\text{-crypt})]_2Ge_9^{2-}$, as well as from the reaction solution. The Raman investigation shows strong bands at 212 cm^{-1} corresponding to the breathing vibration mode of the $\{Ge_9\}$ cluster[24] (cf. Figures S1 and S2 in the Supporting Information).

As alluded to in the structural description above, the Ge_9^{2-} cluster is regarded as a 20-electron *closo* cluster ($2n + 2$ electrons with $n = 9$ yields 20 electrons available for cluster-skeleton bonding) within the Wade's rules formalism, which has been shown to work surprisingly well for main-group clusters (see ref.[25] and references [2–11] in ref.[25]). Alternatively, only considering the valence electron number, each germanium atom carries 4 electrons, and 2 further electrons are obtained from the charge, in total 38 electrons. However, of this total of 38, 18 electrons are expected to reside in electron pairs, one on each germanium atom, leaving 20 electrons for cluster-skeleton bonding. The *closo* cluster is expected to have D_{3h} symmetry, thus that of

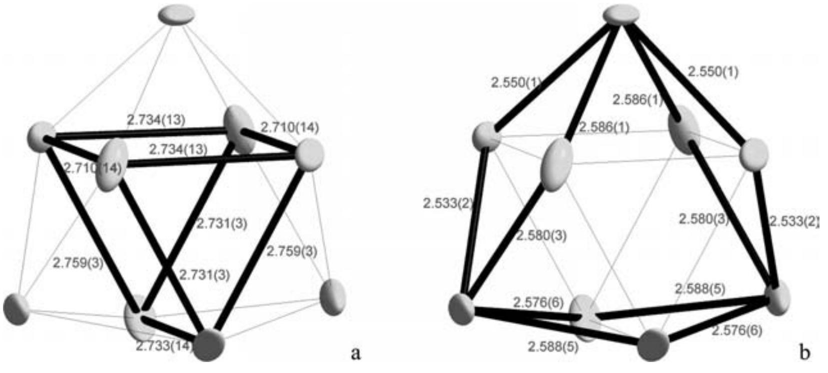

Figure 1. Tricapped trigonal-prismatic shape of the Ge_9^{2-} cluster refined from the data collected at 100 K. The twofold axis of the structure is vertical. Note the neat distribution of distances between the two kinds of atomic positions in the tricapped trigonal prism. The distances within the trigonal prism are all in the range 2.71–2.76 Å (a), and the distances between the trigonal prism and the capping atoms are in the range 2.53–2.59 Å (b).

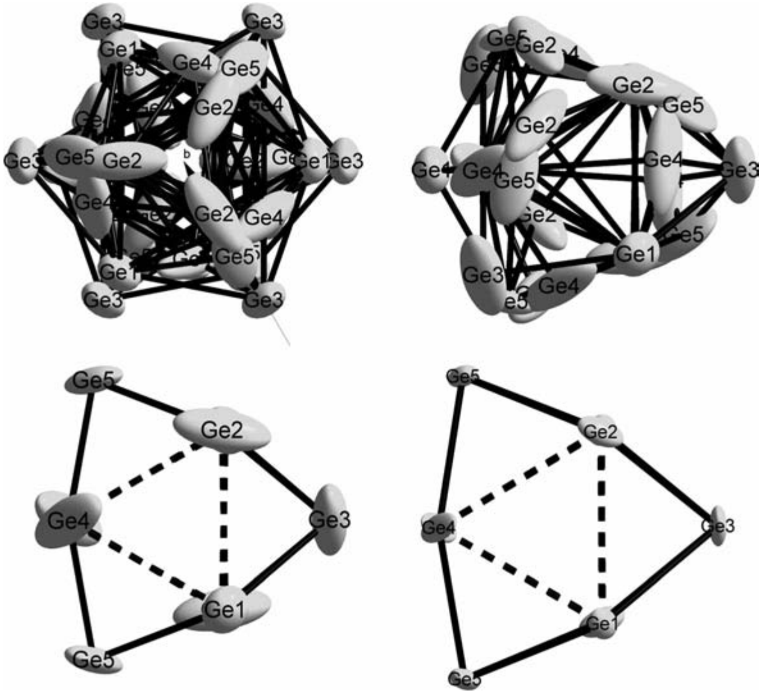

Figure 2. Retrieval of the fully ordered cluster as a partial population of the atomic positions from the structure produced by the refinement of the data collected at 250 K. In all images, the horizontal direction corresponds to the twofold axis of the cluster, i.e. the *a*-axis of the trigonal cell and the *b*-axis of the monoclinic cell, respectively. Top left: Projection along the *c*-axis of trigonal cell of the disordered cluster of the structure refined from the data collected at 250 K. Top right: Same cluster viewed along the pseudo threefold direction of the ordered cluster. Bottom left: Same view as top right, but only selected positions are shown. Bottom right: Ordered cluster in the 100 K structure viewed along the pseudo three-fold direction.

a tricapped trigonal prism as deduced from the structural analysis (vide supra). Just from looking at the number of edges in a tricapped trigonal prism, it is clear that the cluster does not possess a sufficient number of electrons to allow a localized bonding scheme with (2c,2e)-bonds alone. Instead, delocalized bonding should be expected.

Interestingly enough, the quantum chemical calculations identified two different conformers of D_{3h} symmetry. The lowest-energy structure is very similar to the one obtained from the crystallographic study above and the other is about 160 kJ mol^{-1} (1.68 eV) higher in energy. The structure of the lowest-energy conformation is shown in Figure 3. The Ge–Ge distances are similar to the crystallographic ones although slightly longer. This is a common phenomenon for interatomic distances of main-group clusters produced by means of quantum chemical calculations. The calculated distances from the capping atoms to the square faces of the trigonal prism (the corresponding crystallographic distances are given within parentheses) are 2.61 Å (2.56 Å), and the distances within these faces are 2.77 (2.71–2.73 Å; height of the squares) and 2.80 Å (2.73–2.76 Å; within the triangular faces). The coherence between calculated and structural results must be considered excellent. The structure of the higher-energy conformation is more elongated, dominated by short intratriangular bonding (2.56 Å; prismatic faces) and an extended trigonal prism height (3.58 Å). The distance between the prismatic and capping germanium atoms is 2.69 Å. In the following discussion, mainly the bonding scheme of the lowest-energy

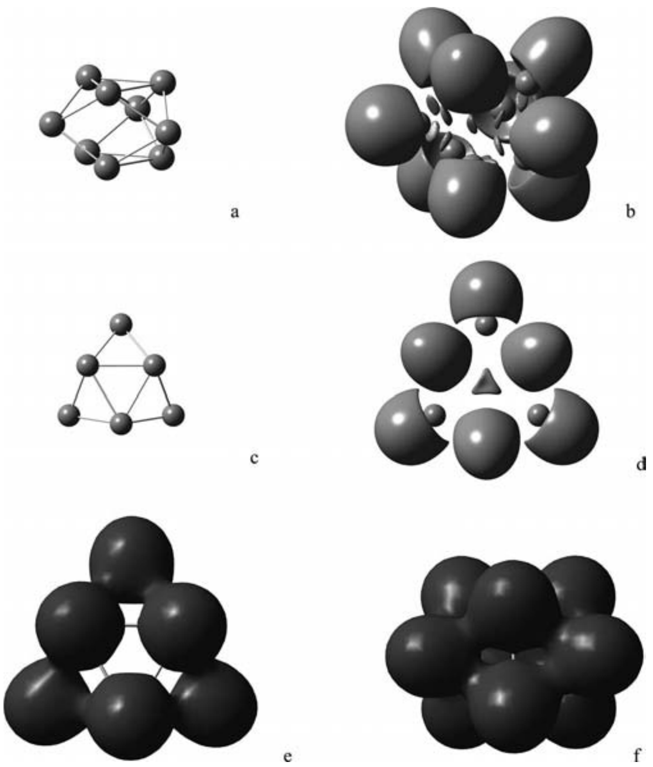

Figure 3. Calculated, lowest-energy conformer of the Ge_9^{2-} structure, represented as a cage structure [(a) and (c)] and the ELF image of the Ge_9^{2-} cluster [(b) and (d); isovalue 0.55]. Top and side view of the total electron density for Ge_9^{2-} [(e) and (f), respectively].

conformation will be discussed. Looking at bond lengths, it is tempting to allocate a bonding scheme similar to that indicated in Figure 1, representing a cage-type of bonding rather than a polygonal one. Even in such a scheme there would be 12 or 15 (including the bonds between prismatic germanium atoms as well) bonds to consider and this is far too many for 20 bonding electrons in the *closo* cluster. An average bond order in the range 0.67–0.83 should thus be expected from simple topological arguments. According to Pyykkö and co-workers, a single Ge–Ge bond is about 2.42 Å.[26] Consequently, it is clear that all Ge–Ge distances in the $Ge_9^{2–}$ cluster are significantly longer, and bond orders smaller than one should be expected. In fact, a natural bond order (NBO) analysis shows that the bond order from a capping germanium atom to its nearest neighbours is about 0.65. A natural bond order population analysis allocates a charge of –0.20 to the capping atoms and –0.23 to the prismatic atoms, also indicating delocalised bonding. Finally, it is notable that the totally symmetric stretching vibration (breathing mode; A_1' symmetry) is 216 cm^{-1}, in excellent agreement with experiment (Figure S1). Calculations also predict a relatively strong Raman band at 177 cm^{-1}, corresponding to an intratriangular (prismatic faces) stretching mode, which may constitute one of the rather strong peaks below 200 cm^{-1} (Figure S1).

In order to gain a deeper insight into the bonding scheme of the $Ge_9^{2–}$ cluster and of the presence of nonbonding electron pairs, electron localisation function analyses (ELF and ELI-D) were executed. The results are shown in Figure 3. The images are dominated by the nonbonding electron pairs on each germanium atom, but the accumulation of electron-pair probability over the two triangular prismatic faces (Figure 3c and d) may be interpreted as two (3c,2e)-bonds. However, the side-view (Figure a and b) reveals electron-pair density accumulated approximately between all capping-to-triangular prism bond vectors, and (2c,2e)-bonds may be inferred. A fully localised bonding scheme of this type between the capping-to-triangular prismatic Ge atoms would, however, require 24 electrons, and thus these interactions must also be delocalised. By considering the number of cluster electrons available [16 electrons, when the four triangular (2c,3e)-electrons have been subtracted], it is necessary to propose a complex multicentre capping-to-triangular prismatic bonding scheme, because 16 electrons cannot be divided by 3 faces nor 12 2c-bonds to give an integer. In conclusion, the bonding scheme of the *closo*-$Ge_9^{2–}$ cluster must be regarded as highly delocalised over the whole cluster. As a curiosity, it can be noted that the energetically less favourable structure (also of D_{3h} symmetry) instead indicates a localised bonding in the triangular faces of the trigonal prism. For comparison, a similar bonding analysis to that made for the $Ge_9^{2–}$ unit was made for the corresponding and better known $Ge_9^{4–}$ cluster by using the same tools and the same level of theory. The $Ge_9^{4–}$ cluster turns out to be computationally more well-behaved in the sense that both structures of D_{3h}, C_{4v} and C_{2v} readily converge into stable conformers. However, the interpretation of the results is less straightforward. From cluster electron bookkeeping rules, we would expect a *nido*-$Ge_9^{4–}$ cluster of C_{4v} symmetry. The energy difference between the C_{4v} and D_{3h} conformers is, however, only 20 J mol^{-1} (*not* kJ mol^{-1}; about 0.0002 eV) and thus essentially negligible. Translated into thermal energy, this energy difference corresponds to a temperature of 2.5 K. The transfer of a D_{3h} cluster into C_{4v} symmetry, or vice versa, requires very small atomic rearrangements and is expected to proceed through a transition state of C_{2v} symmetry. The C_{2v} conformer essentially represents no barrier to transfer. The practical consequence is that the $Ge_9^{4–}$ cluster is expected to be very fluxional even at low temperatures and that it is unlikely that crystallographic determinations can distinguish a single conformer structure even if diffraction data are recorded at 100 K or lower temperatures. This result is analogous to that previously observed for the $Sn_9^{4–}$ clusters.[23]

A comparison between the D_{3h} conformers of the *closo*-$Ge_9^{4–}$ cluster and the corresponding *closo*-$Ge_9^{2–}$ cluster in focus in the present work also indicates that, although the symmetry is the same, the two clusters differ in Ge–Ge distance distributions. The *intra*-triangular (prismatic) Ge–Ge distances of the $Ge_9^{4–}$ cluster is about 0.1 Å shorter than in the $Ge_9^{2–}$ cluster, whereas the *inter*-triangular (height of trigonal prism) is 0.4 Å longer than in the $Ge_9^{2–}$ cluster. Thus, the trigonal prism of the $Ge_9^{4–}$ cluster is a bit thinner and considerably longer than in the $Ge_9^{2–}$ cluster. The distances to the capping Ge atoms are similar in both clusters. In spite of the structural differences, the $Ge_9^{4–}$ cluster exhibits no sign of any (3c,2e)-bonding in the prismatic triangles but a very similar electron-pair density distribution between the capping and prismatic Ge atoms as in the $Ge_9^{2–}$ cluster (as in Figure 3d, e and f). Although topologically different, the bonding in $Ge_9^{4–}$ must be highly delocalised as well.

The topological difference between $Ge_9^{4–}$ and $Ge_9^{2–}$ is also evident when comparing the crystallographic structure determinations of the two. The $Ge_9^{4–}$ unit isolated by Belin et al. in $[\text{crypt-K}^+]_6Ge_9^{2–}Ge_9^{4–}\cdot 2.5en$ is described as having a symmetry close to C_{4v} and a monocapped antiprismatic configuration. As the parallel edges of the trigonal prism are not equal in length, and as the distances between the capping atoms in $Ge_9^{4–}$ are slightly longer than in $Ge_9^{2–}$, $Ge_9^{4–}$ shows a clear deviation from ideal D_{3h} symmetry.

Conclusions

The present work contains results of a detailed structural examination of the compound $[K^+(2,2,2\text{-crypt})]_2Ge_9^{2–}$ containing *closo*-$Ge_9^{2–}$ clusters of (close to) D_{3h} symmetry characterised by extensive electron delocalisation.

Experimental Section

Synthesis: The synthesis was carried out under nitrogen in a glove box. A small 11 × 2 mm reaction vial was used. The K_4Ge_9 precursor[27] was synthesised by means of a solid-state reaction from the stoichiometric mixture of elemental potassium (Merck, 99 %) and germanium (Chempur, 99.9999+ %). The two elements were heated in a sealed niobium tube at 850 °C for 2 h. Ethylenediamine (en) (Fluka, > 99.5%) was carefully dried with Na/K and by using molecular sieves prior to the use in the synthesis. The 2,2,2-crypt (Sigma Aldrich, 98.0%) was used as received. The reaction resulting in the isolation of $[K^+(2,2,2\text{-crypt})]_2Ge_9^{2-}$ was carried out by mixing K_4Ge_9 (50 mg, 0.062 mmol) and 2,2,2-crypt (90 mg, 0.239 mmol) in ethylenediamine (2 mL). After several hours of stirring, undissolved starting material was filtered off. The red-brownish reaction solution was then layered with toluene (0.5–1 mL) for protection against oxidation, and the vial was wrapped in aluminium foil and left. After a few weeks, red-brownish block-like crystals had formed on the walls of the reaction vessel. In the subsequent single-crystal X-ray experiment, the quality of these crystals was proven to be very high.

Single-Crystal X-ray Diffraction: A crystal with well-developed faces was immersed in a droplet of Paratone and mounted on a thin glass fibre. The ensemble was quickly cooled to 100 K in a stream of nitrogen. A full sphere of diffraction data was collected with an Oxford Diffraction Xcalibur3 system by using Mo-K_α radiation. After the completion of the low-temperature measurement, a new measurement was performed at 250 K. This temperature was chosen to ensure that the crystal would remain fixed by the solidified Paratone but still be as close to room temperature as possible. All information pertinent to the data collection is given in Table 1. Whereas the data collected at 250 K refined to a model similar to that of Belin et al.[17] (Table 2), the data collected at low temperature could not be refined, despite automatic indexing producing a unit cell very similar to that of the 250 K measurement ($a = b =$ 11.8 Å, c = 22.4 Å, $\alpha = \beta = 90°$, $\gamma = 120°$). A closer investigation of the reciprocal lattice revealed that the diffraction pattern obtained at 100 K is distinctly different from that at 250 K. For layers with low values of the index *l*, reconstructed reciprocal lattice layers are indistinguishable for the two measurements but for higher values of *l*, individual reflections split up into shamrock-like arrangements, indicating twinning (Figure 4). The splitting may be explained by a small monoclinic distortion of the underlying hexagonal lattice, the unique monoclinic axis being parallel to the trigonal *a*-axis direction. This means that the maximal applicable monoclinic subgroup to the trigonal $P\bar{3}c1$ is $C2/c$. Consequently, the data set collected at 100 K was integrated by using a monoclinic cell, for which the low *l* index reflections represent a complete overlap of the three domains, the intermediate *l* index reflections an incomplete overlap, whereas the high *l* index reflections do not overlap, and diffraction from only one individual was integrated. The structure was solved, without further treatment of the data, in the space group $C2/c$ by using charge flipping,[28,29] as implemented in the program Superflip,[30] and this produced all non-hydrogen atoms in a straightforward fashion. Refinement was carried out by using the Jana2000[31] program. Hydrogen atoms were subsequently introduced by using a riding model. Not unexpectedly for data from a complex twin, extinction correction proved unnecessary. Integration of such a pattern is an intricate problem. In the *hkl* layers close to $l = 0$, the overlap between the different individuals is perfect and integration presents no problem. For *hkl* layers with $l >> 0$ the individuals are well separated and integration again presents no problem. However, for intermediate values of *l*, the incomplete overlap makes evaluation difficult. In the refinement, this leads to a less-than-satisfactory result for residuals [R_f = 8.7%, $R_w(F^2)$ = 18.3%]. The most straightforward way to handle such problems is

Table 1. Crystal data.

100 K Measurement		250 K Measurement	
Crystal data			
$C_{36}H_{72}Ge_9K_2N_4O_{12}$			
M_r = 1484.5			
Mo-K_α radiation			
Z = 4	monoclinic, $C2/c$	Z = 2	trigonal, $P\bar{3}c1$
a = 20.4828(18) Å	μ = 5.15 mm^{-1}	a = 11.9150(6) Å	μ = 5.05 mm^{-1}
b = 11.8105(9) Å	T = 100 K		T = 250 K
c = 22.296(3) Å	0.14 × 0.11 × 0.08 mm	c = 22.3517(15) Å	0.14 × 0.11 × 0.08 mm
β = 91.696(10)°	V = 5391.3(10) Å^3		V = 2748.1(3) Å^3
Data collection			
XCalibur III diffractometer			
Absorption correction: analytical from shape			
15691 reflections with $I > 3\sigma(I)$	R_{int} = 0.154	859 reflections with $I > 3\sigma(I)$	R_{int} = 0.153
T_{min} = 0.592, T_{max} = 0.711	θ_{max} = 33.2°	T_{min} = 0.592, T_{max} = 0.711	θ_{max} = 33.3°
82974 measured reflections	74672 independent reflections	49356 measured reflections	3421 independent reflections
Refinement			
$R[F^2 > 2\sigma(F^2)]$ = 0.066	$wR(F^2)$ = 0.170	$R[F^2 > 2\sigma(F^2)]$ = 0.041	$wR(F^2)$ = 0.077
S = 0.82	$\Delta\rho_{max}$ = 3.13 e Å^{-3}	S = 0.86	$\Delta\rho_{max}$ = 1.13 e Å^{-3}
74672 reflections	$\Delta\rho_{min}$ = –1.63 e Å^{-3}	3421 reflections	$\Delta\rho_{min}$ = –0.78 e Å^{-3}
157 parameters		109 parameters	

Table 2. Comparative table showing the structure as reported by Belin et al.[17] and data from this study at 250 K side-by-side to indicated the similarities. Apart from the need to invoke an additional Ge position, the results are very similar.

	Data from Belin et al.[17]			Data from this study		
Ge1	0.0914(9)	0.0926(9)	0.1618(4)	0.0861(3)	0.0860(3)	0.16329(9)
Ge2	0.1408(5)	0.1396(5)	0.1880(2)	0.1555(3)	0.1614	0.18649(13)
Ge3	0.1928(2)	0	1/4	0.22598(15)	0	1/4
Ge4	0	–0.2297(7)	0.25	0	–0.18098(7)	1/4
Ge5	–	–	–	0.0920(2)	0.0247(3)	0.20698(13)
K	1/3	2/3	0.0423(3)	1/3	2/3	0.04651(4)

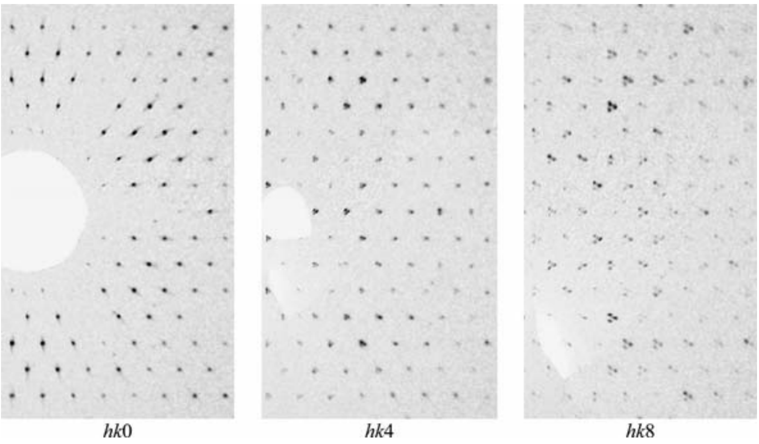

Figure 4. Reconstructed reciprocal lattice images from the 100 K measurement. Note the perfect overlap between individuals in the *hk*0 layer, the well-resolved individuals in the *hk*8 layer and the intermediate situation in the *hk*4 layer.

to eliminate all reflections that are deemed to be problematic. In the refinement of the 100 K data set, reflections in the range *hkl* with $3 \leq |l| \leq 5$ were eliminated after considering the reciprocal lattice sections in Figure 4. The procedure is completely equivalent to introducing a forbidden range of angular separation between reflections and removing all reflections that fall into this category. The residuals from a refinement based on this reduced data set are more satisfactory [$R_f = 6.6\%$, $R_w(F^2) = 13.7$], but the reduced information precludes the possibility of refining the light cryptand atoms by using anisotropic thermal parameters. This is no indication of disorder of the cryptand but only an indication of a decreased effective data-to-parameter ratio. The integration was carried out by using the software Crysalis RED.[32] The integration, as well as the refinement, show that the twinning is unbalanced and hence that the domains are large. Interestingly enough, in the data set that was collected subsequently at 250 K, there is no indication of any cracking of the crystal. The diffraction pattern is that of a high-quality single crystal. This shows that it is possible to cycle the phase transition and possibly even to anneal the low-temperature phase in order to obtain a single-domain specimen. CCDC-792790 and -832455 contain the supplementary crystallographic data for this paper. These data can be obtained free of charge from The Cambridge Crystallographic Data Centre via www.ccdc.cam.ac.uk/data_request/cif.

Computations: Calculations were performed by using the Gaussian 03 program package.[33] All calculations include energy optimisation and evaluation of the total-energy eigenvalues. Both Hartree–Fock (HF) and hybrid density-functional theory (DFT) calculations were performed. The effective core pseudo-potentials (ECPs) and valence basis set for germanium were of MDF10 and (12s12p9d)/[6s6p4d] quality, respectively.[34] Calculations were performed at Hartree–Fock and various density-functional or hybrid density-functional levels in order to verify the general characteristics of the Ge_9^{2-} system. Results presented in the text are taken from hybrid B3PW91 calculations. Electron localisation function densities (ELF and ELI-D) were calculated by using the DGrid 4.5 program.[35]

Supporting Information (see footnote on the first page of this article): Raman data for the compound.

Acknowledgment

We thank the Swedish Research council VR for support.

---

[1] E. Busman, *Naturwissenschaften* **1960**, *47*, 82.
[2] V. Queneau, S. Sevov, *Angew. Chem.* **1997**, *109*, 1818; *Angew. Chem. Int. Ed. Engl.* **1997**, *36*, 1754–1756.
[3] C. Belin, J. Corbett, A. Cisar, *J. Am. Chem. Soc.* **1977**, *99*, 7163–7169.
[4] V. Angilella, C. Belin, *J. Chem. Soc. Faraday Trans.* **1991**, *87*, 203–204.
[5] J. Campbell, G. Schrobilgen, *Inorg. Chem.* **1997**, *36*, 4078–4081.
[6] L. Xu, S. Sevov, *J. Am. Chem. Soc.* **1999**, *121*, 9245–9246.
[7] C. Downie, Z. Tang, A. Guloy, *Angew. Chem.* **2000**, *112*, 346; *Angew. Chem. Int. Ed.* **2000**, *39*, 337–340.
[8] A. Ugrinov, S. Sevov, *J. Am. Chem. Soc.* **2002**, *124*, 10990–10991.
[9] A. Ugrinov, S. Sevov, *Inorg. Chem.* **2003**, *42*, 5789–5791.
[10] J. D. Corbett, P. A. Edwards, *J. Am. Chem. Soc.* **1977**, *99*, 3313–3317.
[11] S. Sevov, J. Goicoechea, *Organometallics* **2006**, *25*, 5678–5692.
[12] T. F. Fässler, *Inorg. Chem.* **1994**, *33*, 5380–5381.
[13] T. F. Fässler, *Coord. Chem. Rev.* **2001**, *215*, 347–377.
[14] J. M. Goicoechea, S. C. Sevov, *J. Am. Chem. Soc.* **2006**, *128*, 4155–4161.
[15] J. D. Corbett, *Chem. Rev.* **1985**, *85*, 383–397.
[16] J. D. Corbett, *Struct. Bonding (Berlin)* **1997**, *87*, 157–193.
[17] C. Belin, H. Mercier, V. Angilella, *New J. Chem.* **1991**, *15*, 931–938.
[18] A. Ugrinov, S. Sevov, *Chem. Eur. J.* **2004**, *10*, 3727–3733.
[19] T. Fässler, M. Hunziker, M. Spahr, H. Leuken, *Z. Anorg. Allg. Chem.* **2000**, *626*, 692–700.
[20] D. Rios, S. Sevov, *Inorg. Chem.* **2010**, *49*, 6396–6398.
[21] S. Ulvenlund, K. Ståhl, L. Bengtsson-Kloo, *Inorg. Chem.* **1996**, *35*, 223–230.
[22] M. Lindsjö, A. Fischer, L. Kloo, *Angew. Chem.* **2004**, *116*, 2594; *Angew. Chem. Int. Ed.* **2004**, *43*, 2540–2543.
[23] J. Rosdahl, T. F. Fässler, L. Kloo, *Eur. J. Inorg. Chem.* **2005**, 2888–2894.
[24] H. G. von Schnering, M. Baitinger, U. Bolle, W. Carrillo-Cabrera, J. Curda, Yu. Grin, F. Heinemann, J. Llanos, K. Peters, M. Somer, *Z. Anorg. Allg. Chem.* **1997**, *623*, 1037–1039.
[25] A. N. Kuznetsov, L. Kloo, M. Lindsjö, J. Rosdahl, H. Stoll, *Chem. Eur. J.* **2001**, *7*, 2821–2828.
[26] P. Pyykkö, M. Atsumi, *Chem. Eur. J.* **2009**, *15*, 186–197.
[27] S. Ponou, T. F. Fässler, *Z. Anorg. Allg. Chem.* **2007**, *633*, 393–397.
[28] G. Oszlanyi, A. Suto, *Acta Crystallogr., Sect. A* **2004**, *60*, 134–141.
[29] G. Oszlanyi, A. Suto, *Acta Crystallogr., Sect. A* **2005**, *61*, 147–152.

[30] L. Palatinus, G. Chapuis, *J. Appl. Crystallogr.* **2007**, *40*, 786–790; http:/superspace.epfl.ch/superflip.

[31] V. Petříček, M. Dušek, L. Palatinus, *The Crystallographic Computing System Jana2000*, Institute of Physics AVCR, Praha, Czech Republic, **2000**.

[32] Oxford Diffraction, *CrysAlis RED*, p171.31.2, **2006**.

[33] M. J. Frisch, G. W. Trucks, H. B. Schlegel, G. E. Scuseria, M. A. Robb, J. R. Cheeseman, J. A. Montgomery Jr., T. Vreven, K. N. Kudin, J. C. Burant, J. M. Millam, S. S. Iyengar, J. Tomasi, V. Barone, B. Mennucci, M. Cossi, G. Scalmani, N. Rega, G. A. Petersson, H. Nakatsuji, M. Hada, M. Ehara, K. Toyota, R. Fukuda, J. Hasegawa, M. Ishida, T. Nakajima, Y. Honda, O. Kitao, H. Nakai, M. Klene, X. Li, J. E. Knox, H. P. Hratchian, J. B. Cross, V. Bakken, C. Adamo, J. Jaramillo, R. Gomperts, R. E. Stratmann, O. Yazyev, A. J. Austin, R. Cammi, C. Pomelli, J. W. Ochterski, P. Y. Ayala, K. Morokuma, G. A. Voth, P. Salvador, J. J. Dannenberg, V. G. Zakrzewski, S. Dapprich, A. D. Daniels, M. C. Strain, O. Farkas, D. K. Malick, A. D. Rabuck, K. Raghavachari, J. B. Foresman, J. V. Ortiz, Q. Cui, A. G. Baboul, S. Clifford, J. Cioslowski, B. B. Stefanov, G. Liu, A. Liashenko, P. Piskorz, I. Komaromi, R. L. Martin, D. J. Fox, T. Keith, M. A. Al-Laham, C. Y. Peng, A. Nanayakkara, M. Challacombe, P. M. W. Gill, B. Johnson, W. Chen, M. W. Wong, C. Gonzalez, J. A. Pople, *Gaussian 03*, Revision C.02, Gaussian, Inc., Wallingford, CT, **2004**.

[34] B. Metz, H. Stoll, M. Dolg, *J. Chem. Phys.* **2000**, *113*, 2563–2569.

[35] M. Kohout, *DGrid*, version 4.5, Radebeul, **2009**.

Received: April 24, 2011